Scanning Electron Microscopy

Volume 1982
Number 1 *1982*

Article 17

1982

A Transport Equation Theory of Electron Scattering

D. J. Fathers
University of Sussex

P. Rez
V.G. Microscopes Ltd.

Electron Beam Interactions With Solids (Pp. 193-208)
SEM, Inc., AMF O'Hare (Chicago), IL 60666, U.S.A.

A TRANSPORT EQUATION THEORY OF ELECTRON SCATTERING

D.J. FATHERS*
School of Mathematical and Physical Sciences
University of Sussex
Falmer, Brighton, Sussex BN1 9QH, U.K.

and

P. REZ
V.G. Microscopes Ltd.
East Grinstead, Sussex, U.K.

ABSTRACT

The use of the Boltzmann transport equation to describe electron scattering in electron microscopy and electron probe microanalysis is discussed. A method of solution is given in which the transport equation is divided into angle and energy intervals. This gives rise to a number of coupled first order differential equations. Separation into forward and backward travelling components of the electron flux distribution enables the correct boundary conditions to be imposed. Solutions are derived which take the form of matrix operators analytic in both depth and target thickness. These matrices allow derivation of other physical quantities such as X-ray or Auger electron production.

Calculations using this method are fast and accurate. Results are presented showing angular distributions of backscattered electrons and the variation of the backscattered fraction with angle of incidence and atomic number. The variations of backscattered, transmitted and absorbed fractions with target thickness are presented. The theory has also been applied to the calculation of the energy distributions of backscattered electrons, energy dissipation and X-ray production as functions of depth and the Auger backscattering factor.

It appears that electron scattering in thick targets is not amenable to treatment using simple models. This is because most of the features of interest are determined by a combination of medium angle scattering ($< 20°$) and large angle scattering (20-90°). Nevertheless certain approximations within the present framework, which describe multiple scattering correctly, can give some useful insights.

Keywords: Backscattered electron distributions, transmitted electron distributions, elastic scattering, inelastic scattering, multiple scattering, transport equation, X-ray production, Auger electron production.

*Present Address:
V.G. Microscopes Ltd.
Charlwoods Road
East Grinstead
Sussex RH19 2JQ, U.K.
Phone 0342-312636

INTRODUCTION

A theoretical description of the scattering of electrons inside solids is desirable for a complete understanding of many aspects of electron microscope image contrast, electron beam microanalysis and electron beam lithography. To calculate image contrast it is necessary to be able to calculate the distribution of backscattered electrons in angle and energy. This information may be combined with the appropriate detector response function to produce a theoretical image which may be directly compared with the experimental one. Similarly, in X-ray or Auger electron microanalysis it is necessary to be able to calculate the X-ray or Auger electron production. This requires knowledge of the electron flux distributions as a function of angle, energy and depth below the sample surface. Finally in electron beam lithography the energy dissipation function must be calculated as a function of at least two spatial dimensions.

Many of these topics are covered in other papers in these proceedings. It is the purpose of this paper to present a theoretical approach to electron scattering using the Boltzmann transport equation.

Previous approaches to electron scattering have been made in one of three ways. Everhart (1960) and Archard (1961) developed simple models starting from the opposite premises that backscattering is due to large angle single scattering or multiple small angle scattering which may be described as diffusion. A more sophisticated example of a diffusion theory is given by Kanaya and Ono (1978). A second method is by simulation of electron trajectories using a Monte Carlo technique (Shimizu et al. (1972), Bishop (1965)). Finally a number of attempts have been made to solve the Boltzmann transport equation describing electron scattering (Spencer (1974), Brown and Ogilvie (1966), Fathers and Rez (1979)).

Monte Carlo methods consider the behaviour of individual electrons. The trajectory of the electron through the solid is calculated step by step assuming it is scattered through randomly determined angles. In most treatments the electron energy at each step is calculated in the continuous slowing down approximation from the Bethe energy loss law. The trajectories of many thousand electrons are calculated to build up the appropriate distribution. More sophisticated treatments dispense with the continuous slowing down approximation by using random numbers to determine the path lengths and energy losses (Reimer and Krefting (1975)).

The disadvantage of Monte Carlo techniques is the large

LIST OF SYMBOLS

f	=	Distribution function ($m^{-6}s^3$)
x,y,z	=	Spatial co-ordinates (m)
t	=	Time (s)
v_x, v_y, v_z	=	Velocity co-ordinates (m s^{-1})
σ	=	Scattering probability (m^{-1})
S	=	Source strength ($m^{-7}s^4$)
Θ,Φ	=	Zenith and Azimuth angles
E	=	Electron energy (Joules)
I	=	Electron flux ($m^{-5}s^2$)
α	=	Scattering angle
s	=	Path length (m)
F_r, A_r	=	r^{th} Legendre polynomial coefficients
P_r	=	r^{th} Legendre polynomial
σ_T	=	Total scattering probability (m^{-1})
I_F, I_B	=	Forward and backward travelling electron flux ($m^{-5}s^2$)
b,c	=	Legendre coefficients of I_F, I_B
M,N	=	Number of angle, energy segments
E_0	=	Incident electron energy (Joules)
i,j	=	Angle subscripts
m,n	=	Energy subscripts
A	=	Scattering Matrix (m^{-1})
A_F, A_B	=	Partitioned A (m^{-1})
R	=	Reflection operator
V,X,Λ	=	Eigenvector and eigenvalue matrices
V1,V2,λ	=	Partitioned V and A
I_0	=	Incident electron flux ($m^{-5}s^2$)
T	=	Transmission operator
η	=	Total backscattered electron yield
$\Delta I_B, \Delta R, \Delta A$	=	Small variation in I_B,R,A
Z	=	Atomic number
e	=	Electronic charge (Coulombs)
N	=	Atomic density (m^{-3})
J	=	Ionization potential (Joules)
ϵ_0	=	Permittivity of free space (Farad m^{-1})
η_B	=	Integrated backscattered fraction
Θ_0	=	Incident electron angle (to surface normal)
ϱ	=	Target density (km^{-3})
Ω	=	Solid angle (steradians)
r_B	=	Electron range (m)
η_T	=	Integrated transmitted fraction
η_A	=	Integrated absorbed fraction
Φ	=	Normalized rate of X-ray production (s^{-1})
μ	=	X-ray absorption coefficient
Θ_T	=	X-ray detector take-off angle
r	=	Auger backscattering factor
B_m, D_m	=	Fourier coefficients of I and σ
υ,r,a	=	Matrix elements in forward backward model
T_{mn}	=	Supermatrix eigenvector element

amount of computer time taken to obtain statistically significant results. This is an even more serious problem when calculating small effects unless correlated sampling is used (Jakubovics and Fathers (1978)).

The Boltzmann equation has been employed in transport problems in many different branches of physics including neutron scattering in nuclear reactors, radiative transfer in stars and beta ray penetration of solids. A variety of mathematical techniques have been developed in these fields. In many cases the treatments are appropriate to neutron scattering for which the scattering cross section is nearly isotropic. Electron scattering cross sections, on the other hand, are extremely anisotropic and these treatments cannot be used.

Furthermore, many early methods were derived before large computers were available. As a result complex analytic approximations were used that were often not accurate. In recent years the main transport equation calculations have been those of Brown, Wittry and Kyser (1969), Bennett and Roth (1972), Spencer and Humphreys (1980) and Fathers and Rez (1979).

The most widely applicable approach is that given by Fathers and Rez in which semi-analytic solutions were obtained as matrix operators. This work was, however, limited to semi-infinite targets. In this paper new results are given which are analytic in depth and target thickness. The emphasis throughout this paper is on the method of calculation and the ways in which it may be applied to a variety of problems.

TRANSPORT EQUATION AND ITS FORMULATION

Transport equation methods may be formulated directly in terms of a probability distribution function f. f is a function in a phase space defined by three position variables x, y and z, three velocity variables v_x, v_y and v_z and the time t. A point in phase space is therefore described by the position vector $\underline{r}$, the velocity vector $\underline{v}$ and t. The probability of finding an electron in the element of phase space $d^3\underline{r}$, $d^3\underline{v}$, dt centred on $\underline{r}$, $\underline{v}$, t is given by $f(\underline{r},\underline{v},t,)d^3\underline{r}\, d^3\underline{v}\, dt$. The difference between various transport equations lies in firstly the way in which phase space is divided into elements and secondly the restrictions on which regions of the space are accessible.

The transport equation is essentially an equation of continuity which ensures that all particles are accounted for. Consider the rate at which electrons flow through the element of space shown in Figure 1. For a velocity v_x, the change in f in a time dt is

$$v_x \frac{\partial f}{\partial x}$$

Similar terms are derived for y and z. In the absence of scattering the total derivative with respect to time is zero, therefore

$$\frac{\partial f}{\partial t} + \underline{v} \cdot \nabla f = 0 \qquad 1$$

which is simply, as expected, the equation of continuity.

Two situations may lead to a modification of this equation. Particles may be scattered within the volume element; that is, a particle may enter the element with a velocity $\underline{v}$ and emerge with a different velocity $\underline{v}'$, or may enter the element with a velocity v′ and emerge with a velocity $\underline{v}$. The change in f due to the first process is simply

$$- \int v\sigma(\underline{v}', \underline{v}) \quad f(\underline{r},\underline{v},t) \quad d^3\underline{r} \quad d^3\underline{v}',$$

and due to the second process is

$$\int v' \ \sigma(\underline{v},\underline{v}') \quad f(\underline{r},\underline{v}', t) \quad d^3\underline{r}\, d^3\underline{v}',$$

where $\sigma(\underline{v},v')$ is the probability of scattering per unit length from velocity $\underline{v}$ to $\underline{v}'$. The rate of change in f due to a source of strength S is

$$v\, S(\underline{r},\underline{v},t).$$

Collecting all these terms together we have the complete general transport equation:

$$\frac{\partial f}{\partial t} + \underline{v}\cdot\nabla f = \int v' \ \sigma(\underline{v},\underline{v}') \ f(\underline{r},\underline{v}', t) d^3\underline{r}\, d^3\underline{v}' + \int v \ \sigma(\underline{v}',\underline{v}) \ f(\underline{r},\underline{v},t) \ d^3\underline{r}\, d^3\underline{v}' + v\, S(\underline{r},\underline{v},t). \qquad 2$$

In many cases of interest equation 2 may be simplified. Firstly, only steady state solutions for f are required so that

$$\frac{\partial f}{\partial t} = 0$$

and f is not a function of t. In a smaller number of cases solutions are required for planar semi-infinite specimens or targets. Figure 2 defines the co-ordinate system which will be used. In this scheme the variables x and y may be suppressed.

In the present work we also choose to express the velocity vector in terms of Θ and Φ and its length in terms of the scalar energy variable E. It is also convenient to rewrite equation 2 in terms of an angular flux density per unit area $I(z,\Theta,\Phi,E)$ defined by

$$I(z,\Theta,\Phi,E) = vf(z,\Theta,\Phi,E) \qquad 3$$

This equation becomes, neglecting the source term

$$\cos\Theta\frac{dI}{dz}(z,\Theta,\Phi,E) = \int\Big[\sigma(\Theta,\Phi,E;\Theta',\Phi',E)\ I(z,\Theta',\Phi'E') - \sigma(\Theta',\Phi',E';\Theta,\Phi,E)\ I(z,\Theta,\Phi,E)\Big] \sin\Theta' d\Theta'\, d\Phi'\, dE' \qquad 4$$

A further simplification results from the fact that the scattering cross section σ depends on the square of the difference in velocities.

$$(\underline{v} - \underline{v}')^2 = v^2 + v'^2 - 2vv'\cos\alpha \qquad 5$$

where α is the angle between $\underline{v}$ and $\underline{v}'$, and

$$\cos\alpha = \cos\Theta\cos\Theta' + \sin\Theta\sin\Theta'\cos(\Phi - \Phi') \qquad 6$$

This means that the integral over Φ' is simply a convolution and it can be shown (see Appendix A) that this leads to a direct solution for the azimuthal variation in a Fourier series.

The equation for the first Fourier coefficient (hereafter I) is written,

$$\cos\Theta\frac{dI}{dz}(z,\Theta,E) = \int\int\Big[\sigma(\Theta,E;\Theta',E')\ I(z,\Theta',E') - \sigma(\Theta',E';\Theta,E)\ I(z,\Theta,E)\Big]\sin\Theta'\, d\Theta'\, dE' \qquad 7$$

where σ is now the first Fourier coefficient of the scattering probability.

This equation is similar to those considered in previous treatments, however the most important difference is that no continuous energy loss or small angle approximations have been made.

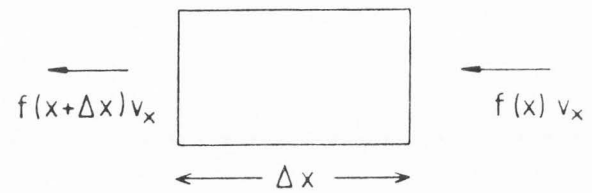

Fig. 1. Schematic diagram showing flow through an element in phase space (here shown in one dimension only).

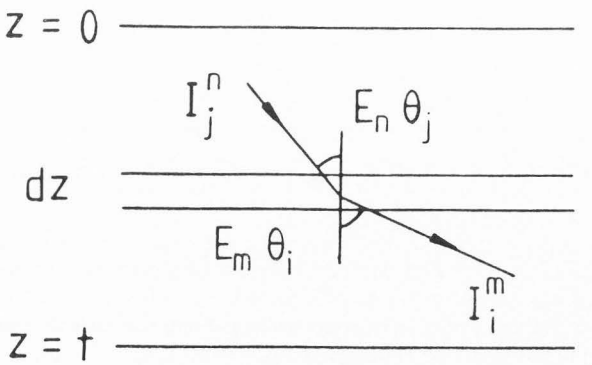

Fig. 2. Schematic diagram showing target and co-ordinate system.

PREVIOUS METHODS OF SOLUTION

It is useful to compare the present approach with other methods used in calculations of electron scattering. Rather than discuss the details of these methods the emphasis will be on the physical meaning of the ideas proposed.

With the exception of Dashen (1964) all methods explicitly involving a transport equation use the integrated path length s rather than energy as a variable. If a continuous energy loss law (for example the Bethe law) is assumed then the two formulations are equivalent. Equation 7 becomes,

$$\cos\Theta\frac{\partial I}{\partial z} + \frac{\partial I}{\partial s} = \int[\sigma(\Theta,\Theta')\ I(\Theta') - \sigma(\Theta',\Theta)I(\Theta)]\, d\Theta' \qquad 8$$

Using path length as a variable can lead to difficulties in formulating a solution to the transport equation. The reason for this is that any electron must have a path length greater than its depth so that the path length is related to the depth. The energy of an electron, on the other hand, can take any value less than the incident energy at any depth.

Of course it is only an advantage to introduce the path length variable to replace the energy variable. In this case there is an implicit assumption that energy loss is not a stochastic process but takes place continuously. Furthermore since there is now a definite path length associated with each energy, there is a maximum value corresponding to a complete loss of energy.

This neglects the phenomenon of straggling which describes the observation of a distribution of energies at a fixed path length, or, conversely a distribution of path lengths at a fixed energy. The present treatment provides a framework within which straggling may be accounted for, although it is likely that in the majority of calculations the energy steps may be too coarse and the straggling may therefore be exaggerated.

One of the first approaches to solving the Boltzmann equation was that of Bethe, Rose and Smith (1938). They reduced the integro-differential transport equation to a partial differential equation called the Fokker-Planck equation. The term $I(\Theta', \Phi', z)$ is expanded to second order in scattering angle. The integral on the right hand side of the transport equation can then be evaluated to give

$$x\frac{\partial I}{\partial z} = \frac{1}{\lambda}\frac{\partial}{\partial x}(x^2\frac{\partial I}{\partial x}), \text{ where } x = \cos\Theta \qquad 9$$

λ, the transport mean free path is given by

$$\frac{1}{\lambda} = \frac{1}{2}\int_0^{\pi}(1 - \cos\alpha)\,\sigma(\alpha)\sin\alpha\,d\alpha \qquad 10$$

This equation is no easier to solve with the correct boundary conditions for backscattering than the original equation. This approximation will be a good one for very small scattering angles. It has been used in a variety of ways by different authors.

Brown and Ogilvie (1966) and later Brown, Wittry and Kyser (1969) used this equation with the path length variable incorporated as follows, to calculate X-ray production.

$$x\frac{\partial I}{\partial z} + \frac{\partial I}{\partial s} = \frac{1}{\lambda(s)}\frac{\partial}{\partial x}(x^2\frac{\partial I}{\partial x}) \qquad 11$$

They set up a three-dimensional grid in path length, angle and depth. The coupling between the neighbouring elements was derived using a finite differences form of equation (11). A single scattering scheme was used very close to the surface and the diffusion form of the Fokker-Planck equation was used for large s. Bennett and Roth (1972) used the same scheme to calculate secondary electron production. Strickland and Bernstein (1976) solved both the Fokker-Planck and the full elastic transport equation to study auroral electron spectra. They found, as might be expected, the Fokker-Planck equation gave accurate results when multiple small angle scattering was dominant.

In many of the early papers the electron distribution function and the cross section were expanded in Legendre polynomials:

$$I(z,\Theta) = \sum_r F_r(z)P_r(\cos\Theta) \qquad 12$$

$$\sigma(\Theta,\Theta') = \sum_r A_r P_r(\cos\Theta)P_r(\cos\Theta') \qquad 12$$

or more generally in spherical harmonics (e.g. Lewis (1950)). The transport equation becomes, where σ_T is the total elastic cross section,

$$\left(\frac{r+1}{2r+3}\right)\frac{dF_{r+1}}{dz} + \left(\frac{r}{2r-1}\right)\frac{dF_{r-1}}{dz} = \left(-\sigma_T + \frac{2A_r}{(2r-1)}\right)F_r \qquad 13$$

It is therefore tridiagonal in form. However if the $\cos\Theta$ on the left hand side of the equation is approximated by 1, then a simpler equation results,

$$\frac{dF_r}{dz} = \left(-\sigma_T + \frac{2A_r}{(2r-1)}\right)Fr \qquad 14$$

which has a solution of the form,

$$F_r(z) = \exp\left(\left(-\sigma_T + \frac{2A_r}{(2r-1)}\right)z\right)F_{r(0)} \qquad 15$$

This equation was first derived by Goudsmit and Saunderson (1940). As pointed out by them this is the exact distribution as a function of path length. The approximation may be a reasonable one for forward elastic scattering up to 20 or 30°, but backscattering cannot be accounted for due to the omission of the $\cos\Theta$. However this equation has been used as a means of speeding up Monte Carlo calculations (see e.g. Shimizu et al., 1972).

Lewis (1950) made no small angle approximation to the transport equation given in equation (8). This equation may be formally solved, however it is difficult to apply the correct boundary conditions.

Lewis (1950) and subsequently L.V. Spencer (1955) could only calculate the spatial moments of distributions in an infinite target with the source at the centre. Physically this allows particles scattered into the half space behind the source to be re-scattered into the sample. This procedure would only be appropriate to a semi-finite target if the backscattering were small.

The boundary conditions can be imposed in two ways. By using the fact that the odd or even Legendre polynomials form a complete set of orthogonal functions in either half space the forward and backward travelling flux distributions may be expanded separately,

$$I_F = \sum_r b_{2r+1}P_{2r+1}(\cos\Theta)$$

and

$$I_B = \sum_r c_{2r+1} P_{2r+1} (\cos \Theta) \qquad 16$$

The boundary conditions lead to simple equations involving coefficients b and c (see e.g. Jacob (1973)).

An alternative method is to use a discrete ordinate scheme (see e.g. Case and Zweifel (1967)). The boundary conditions may then be applied as in the present treatment. The Chandrasekhar method (Chandrasekhar, (1950)) uses Gaussian quadrature for the integration of the right hand side of the transport equation. This is similar to the method presented here but the angular intervals are related to the roots of the Legendre polynomials. Wang and Guth (1951) showed that this procedure is equivalent to the Legendre polynomial method. The most generally used method in calculating neutron flux distribution is the S_N method due to Carlson (see Case and Zweifel (1967)) in which the integral is evaluated by Simpsons rule. This procedure is very convenient for near isotropic scattering as occurs in neutron transport.

The electron scattering cross section is extremely anisotropic. Furthermore the electron source functions of interest are also usually highly anisotropic. This means that many polynomials may be required to represent these functions sufficiently accurately. In his calculations of distributions of multiple scattering in foils Jacob (1973) found that 50 polynomials were needed to specify a function with an angular half width of 4°. At large path lengths the scattering and the flux distribution become much more isotropic and only a few polynomials are required. It is in this regime that it is appropriate to talk of diffusion.

PRESENT METHOD OF SOLUTION

Following Dashen (1964) and J.P. Spencer (1974) equation (7) is cast in matrix form by re-writing the integrals as summations. The angular range of Θ from 0 to π is divided into 2M intervals of size $d\Theta$. 2M is an even integer to ensure that no interval spans $\pi/2$. The energy range from 0 to E_0 is divided into N intervals of width dE thus setting up N energy 'levels'. The highest level is E_0 and the lowest is dE. It is not necessary to subdivide the variable ranges in this way, though this procedure has been used in the majority of calculations.

Equation (7) may now be written:

$$\cos \Theta_i \frac{dI}{dz}(z,\Theta_i,E_m) = \sum_{nj} \left[\sigma(\Theta_i,E_m,\Theta_j,E_n)\, I(z,\Theta_j,E_n) - \sigma(\Theta_j,E_n;\Theta_i,E_m)\, I(z,\Theta_i,E_m) \right] \sin \Theta_j \, d\Theta_j \, dE_n \qquad 17$$

which can be expressed more conveniently as

$$\frac{dI_i^m}{dz} = \sum_{nj} A_{ij}^{mn} I_j^n \qquad 18$$

with the following definitions

$$I_i^m = I(z,\Theta_i,E_m)$$

$$A_{ij}^{mn} = \sigma(\Theta_i,E_m;\Theta_j,E_n) \sin \Theta_j \sec \Theta_i \, d\Theta_j \, dE_n - \delta_{ij} \sum_{nj} \sigma(\Theta_{,},E_n;\Theta_I,E_m) \sin \Theta_j \sec \Theta_i \, d\Theta_j \, dE_n \qquad 19$$

where δ_{ij} is the Kronecker delta. This is just a large system of first order coupled differential equations. The coupling matrix is a supermatrix, that is, a matrix whose elements are themselves matrices.

The superscripts refer to different energy states and the subscripts refer to different angles so that A_{ij}^{mn} is the matrix element denoting scattering from energy E_n and angle Θ_j to E_m and Θ_i, and similarly I_i^m is the flux density of electrons with energy E_m, travelling at an angle Θ_i.

There are now some simplifying assumptions which may be made. First of all, electrons can only lose energy, so that $E_n \geq E_m$ or $n \leq m$. This means that the energy supermatrix is lower triangular, i.e. all the elements above the main diagonal are zero. Secondly it is a reasonable approximation, and one made in most electron scattering calculations, to assume that electrons are inelastically scattered from one energy level to the next. This means that the energy supermatrix becomes bi-diagonal and can be shown as

$$\frac{d}{dz} \begin{pmatrix} I_0 \\ I_1 \\ I_2 \\ . \end{pmatrix} = \begin{pmatrix} A^{00} & 0 & 0 \\ A^{10} & A^{11} & 0 \\ 0 & A^{21} & A^{21} \\ . & 0 & . \end{pmatrix} \begin{pmatrix} I_0 \\ I_1 \\ I_2 \\ . \end{pmatrix} \qquad 20$$

The matrices on the diagonals, the A^{mn} represent elastic scattering and their diagonal terms include the loss of electrons from the given state to all other energies and angles as shown by equations (19). The A^{mn} matrices below the diagonal represent inelastic scattering. It is often assumed that the angular deflections accompanying inelastic scattering are small enough to be neglected. In this case the A^{mn} are diagonal matrices.

If equation (20) is written in supermatrix notation we obtain

$$\frac{d\mathbf{I}}{dz} = \mathbf{A}\,\mathbf{I} \qquad 21$$

Although Dashen (1964) segmented in the angle and energy variables he attempted to solve a non-linear equation. The relationship between this equation and the more normal linear one presented here is given by Bellman et al. (1960). If the scattering matrix **A** were written in a slightly different form, then

$$\mathbf{A} = \begin{pmatrix} A_F & A_B \\ -A_B & -A_F \end{pmatrix} \qquad 22$$

where A_F is a lower triangular supermatrix representing forward scattering through angles less than 90° and A_B is also a lower triangular supermatrix representing backward scattering through angles greater than 90°.

The non-linear equation could then be written

$$\frac{dR}{dt} = A_B + A_F R + R A_F + R A_B R \qquad 23$$

where t is the sample thickness.

If **I** is also partitioned into forward and backward parts, then

$$\mathbf{I} = \begin{pmatrix} I_F \\ I_B \end{pmatrix} \qquad 24$$

and R is defined by the equation

$$I_B(0) = R I_F(0) \qquad 25$$

so R gives the backscattered flux directly. Dashen derived the non-linear equation by an 'invariant' argument applicable only to bulk targets for which the derivative in equation (23) is zero. However he was unable to find the general solution for R. The present solution can be shown, however, to also be a solution of equation (23) (see Appendix B).

The details of the present method of calculation can be illustrated by using the simplified model with a single energy loss (or absorption) in which the energy of an electron is reduced from its initial energy E_0 to zero. The equation may be written

$$\frac{dI_0}{dz} = A^{oo} I_0 \qquad 26$$

where A^{oo} is an ordinary matrix. This equation has the solution

$$I_0(z) = \exp(A^{oo} z) . I_0(0) \qquad 27$$

The exponential of a matrix can be evaluated by expressing the matrix in terms of its eigenvectors V and eigenvalues Λ. Then, dropping the subscripts and superscripts,

$$I(z) = V \exp(\Lambda z) V^{-1} . I(0) \qquad 28$$

If only one angle in each 90° interval is considered the equation becomes similar to the forward backward theories given by Spencer et al. (1972), Liljequist (1977). However Spencer neglected inelastic scattering and therefore electrons could only be 'absorbed' by transmission through a thin sample instead of by loss of energy. If inelastic scattering is included this simple model can give striking results (see Appendix C).

The general solution proceeds by partitioning with respect to forward and backward scattering as outlined above. The symmetry of matrix A is reflected in the symmetry of its eigenvectors and eigenvalues and equation (28) may be written:

$$\begin{pmatrix} I_F(z) \\ I_B(z) \end{pmatrix} = \begin{pmatrix} V_1 & V_2 \\ V_2 & V_1 \end{pmatrix} \begin{pmatrix} \exp \lambda z & 0 \\ 0 & \exp -\lambda z \end{pmatrix} \begin{pmatrix} V_1 & V_2 \\ V_2 & V_1 \end{pmatrix}^{-1} \begin{pmatrix} I_F(0) \\ I_B(0) \end{pmatrix} \qquad 29$$

The boundary conditions may now be applied, for a sample of thickness t,

$$I_F(0) = I_0, \qquad I_B(t) = 0 \qquad 30$$

where I_0 is the incident electron current density.

Simple algebraic manipulation gives the key formulae for I_F, I_B which are analytic in z and t,

$$\begin{aligned} I_F(z,t) = {} & [(V2.\exp -\lambda z.V2^{-1} - V1.\exp -\lambda(t-z). \\ & V2^{-1}.V1.\exp -\lambda t.V2^{-1}) \\ & \times (1 - V1.\exp -\lambda t.V2^{-1}V1.\exp -\lambda t. \\ & V2^{-1})^{-1}] I_0 \end{aligned}$$

$$\begin{aligned} I_B(z,t) = {} & [(V1.\exp -\lambda z.V2^{-1} - V2.\exp -\lambda(t-z).V2^{-1}. \\ & V1.\exp -\lambda t.V2^{-1}) \\ & \times (1 - V1.\exp -\lambda t.V2^{-1}V1.\exp -\lambda t. \\ & V2^{-1})^{-1}] I_0 \end{aligned} \qquad 31$$

Of particular interest are the electron currents variation with depth in a semi infinite (bulk) sample. From above,

$$I_F(z) = [V2.\exp -\lambda z.V2^{-1}] I_0$$

$$I_B(z) = [V1.\exp -\lambda z.V2^{-1}] I_0 \qquad 32$$

and $$I_B(0) = [V1.V2^{-1}] I_0$$

where of course $I_B(0)$ represents the backscattered (i.e. re-emergent) electron distribution sought by Dashen.

The generalization to many energy levels leads to identical expressions to those quoted above, however V1, V2 and Λ are then supermatrices. The method of achieving this is outlined in Appendix D.

OPERATOR FORMALISM

In a general way the matrices used above may be thought of as operators. For example the operator R, the reflection operator, already mentioned, signifies operations which may

be performed on an incident current distribution to result in the backscattered or reflected current distribution. Similarly a transmission operator T may be defined, then,

$$I_B(t) = R(t).I_0$$
$$I_F(t) = T(t).I_0 \qquad 33$$

The usefulness of these equations lies in the way in which they can lead to new results.

Some of the first calculations of electron scattering by Lewis (1950) considered scattering in an infinite medium. This is actually appropriate to scattering by a gas target in which it is possible to have an embedded source. Consider the situation shown in Figure 3(a). The source I_0 is incident on the plane $z = 0$. The target boundaries are at $z = t_1$ and $z = t_2$ and the reflection and transmission operators for the two regions of the target are R_1, T_1 and R_2, T_2 respectively. For continuity at the boundary $z = 0$, we must have,

$$I_F(0) = I_0 + R_1 I_B(0)$$
$$I_B(0) = R_2 I_F(0) \qquad 34$$

which gives for I_B, I_F

$$I_B(0) = R_2(1 - R_2R_1)^{-1} I_0$$
$$I_F(0) = (1 - R_2R_1)^{-1}.I_0 \qquad 35$$

The total current incident on the forward half space is just $I_F(0)$, and that incident on the backward half space is $I_B(0)$. Any distributions derived in this paper can therefore be post multiplied by $(1 - R_2R_1)^{-1}$ or $R_2(1 - R_2R_1)^{-1}$ to give the corresponding distributions for the infinite medium as described here. This provides the relation between the results of L.V. Spencer (1951) and later of Bishop (1967) and the present results.

A similar problem is the case of a two-layer target shown in figure 3(b), for which the result is simply,

$$I_F = (1 - R_2R_1)^{-1} T_1 I_0$$
$$I_B = R_2(1 - R_2R_1)^{-1} T_1 I_0 \qquad 36$$

a result which is easily extended for multiple layers.

Another use for this type of approach is in the calculation of small changes in electron scattering such as magnetic contrast in the scanning electron microscope. Here Monte Carlo techniques are at a serious disadvantage due to the large amount of computer time required to obtain statistically significant results unless correlated sampling techniques are used (Jakubovics and Fathers (1978)).

Using operator methods, from equation (33)

$$I_B(0) = R\, I_0$$

and therefore the variation in I_B is

$$\Delta I_B(0) = \Delta R.I_0 + R.\Delta I_0 \qquad 37$$

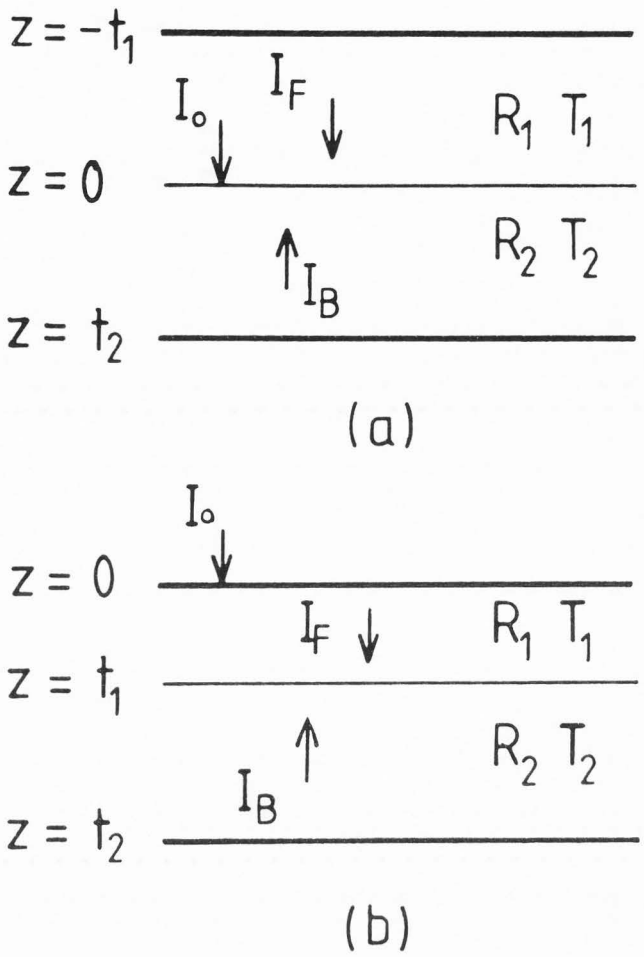

Fig. 3. (a) Diagram showing the geometry for an embedded source I_0. The target extends from $z = -t_1$ to $z = t_2$. (b) Diagram showing the geometry of a two layer target.

The second term describes changes in incident current and is of no interest and for a bulk sample

$$\Delta R = \Delta V1.V2^{-1} + V1\Delta(V2^{-1})$$

and

$$\Delta(V2^{-1}) = -V2^{-1}.\Delta V2.V2^{-1}$$
$$\Delta R = (\Delta V1 - V2^{-1}.\Delta V2)V2^{-1} \qquad 38$$

The small changes in V1 and V2 can be derived from the changes in the scattering matrix ΔA using perturbation theory. This will be described in detail in a forthcoming publication.

COMPUTATIONAL DETAILS

In principle, any scattering cross section can be used in this theory. For the calculations described in this paper a screened Rutherford cross section was used to describe elastic scattering. In this case the Fourier coefficients may be calculated

analytically using calculus of residues. The result for the first coefficient (corresponding to cylindrical symmetry) is, for the off-diagonal elements of the matrix A^{mm},

$$A_{ij}^{mm} = \frac{2\pi Z^2 e^4 N(1 - \cos\Theta_i \cos\Theta_j)}{4E_m^2 c^2 |\cos\Theta_i - \cos\Theta_j|^3} \qquad 39$$

where N is the atomic density and Z is atomic number.

For the inelastic scattering cross section an effective cross section was derived from the Bethe energy loss law such that mean-rate of energy loss was correctly described, i.e.

$$\sigma(\Theta_i,E_n;\Theta_i,E_n)(E_n - E_m) = \frac{dE}{ds}(\bar{E}) \qquad 40$$

where $$\bar{E} = \frac{E_n + E_m}{2}$$

The result is,

$$A_{ii}^{mn} = \frac{4\pi Z e^4 N}{(E_n^2 - E_m^2)c^2} \log\left(\frac{1.166\,\bar{E}}{J}\right) \qquad 41$$

where J is the mean ionization potential, and $c = 4\pi\epsilon_0$.

The number of angular segments M and the number of energy levels N needed for convergence of the solution has been investigated. For integrated quantities such as the total backscattered electron yield, η, the result converges very rapidly for $M \geq 10$ and is not particularly sensitive to the value of N. Angular distributions converge at the same value of M for any value of N. Backscattered electron energy distributions converge reasonably well for N = 5 to 10, although increasing N causes the peak in the distribution to become sharper.

For the details of differential distributions in energy and angle larger values of M and N may be required but it has been found that calculations up to M = 40 and N = 40 are perfectly practicable. It is clear, however, that in the present approximation N should not be increased without limit. The separation of energy levels dE should not be smaller than J, indeed it is quite possible that this is precisely the value required.

Another attractive possibility is to use 'energy levels' which reflect the true nature of inelastic scattering. Both of these are currently being investigated.

The program has been run on a variety of computers. Typical times for execution range from about 1 second on a CDC 7600 using a high level of optimization to about 5 minutes on a PDP 11-03 for M = 5 and N = 10. However, it must be stressed that, as formulated, the program computes simultaneously a family of results for M different angles of incidence and N different incident energies.

RESULTS AND DISCUSSION

Any theory of electron scattering in thick targets must be able to predict certain observable features of the scattered electron distributions in order to be considered useful in predicting features not directly measurable such as the distributions inside the solid. In this section the results of calculations are presented and compared with the relevant experimental results.

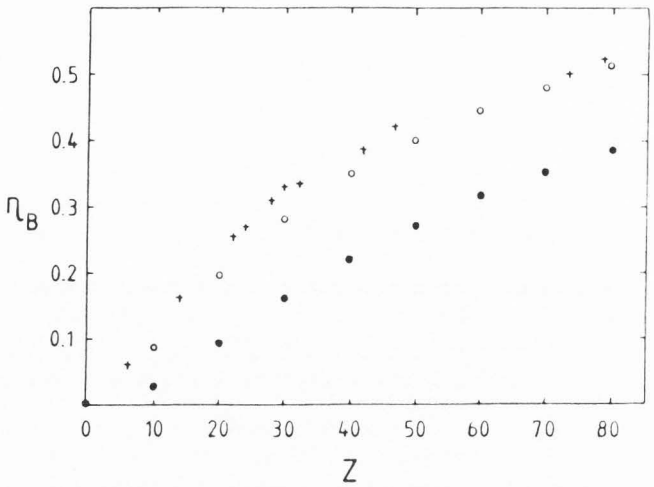

Fig. 4. Backscattered fraction η_B as a function of Z. Crosses represent experimental points. Open circles full calculation. Solid circles for scattering by 20° or less.

Figure 4 shows the results of single energy loss calculations of the integrated backscattered fraction, η_B, as a function of atomic number Z. The calculations were performed for an incident electron energy E_0 = 30 keV and an incident electron angle $\Theta_0 = 0$ (i.e. normal incidence). The target density was assumed to be $\varrho = 0.234\ Z\ gm.cm^{-3}$ and the mean ionization potential J was assumed to be J = 11.5Z in eV. The agreement between the calculated points (open circles) and the experimental points from Bishop (1966) (crosses) is good. The discrepancies may be due to the assumed variations of ϱ and J.

The solid circles show the results of a similar calculation in which only scattering through angles of 20° or less is allowed. This is done by setting the $A_{ij} = 0$ for $j > i + k$ and $i > j + k$ so that the matrix A consists of a non-zero diagonal band of width 2k + 1 elements. This gives rise to values of η_B which are about 30% of the experimental value for low Z and up to about 80% of the experimental value for high Z. When k is varied to allow scattering up to 90° the calculated values of η_B are within a few per cent of the experimental values. Changes in the screening parameter have little effect on these results. This seems to indicate that a large number of medium angle scattering events dominate η_B and that the details of the cross section for very small angles or very large angles are relatively unimportant.

Figure 5 shows the results of a single energy loss calculation of η_B as a function of angle of incidence Θ_0. The calculations were performed for aluminium, copper and gold with E_0 = 30 keV. The results show that η_B increases monotonically with Θ_0 from a minimum at $\Theta_0 = 0$, which is dependent, to a value close to 1, which is more or less independent of Z at Θ_0 close to 90°. This trend is well known and is supported by experimental work (e.g. Kanter (1957)) and other calculations (e.g. Shimizu et al. (1972)).

Fig. 5. Backscattered fraction η_B versus angle of incidence Θ_0 for 30 keV incident electrons.
Curve a; gold
Curve b; copper
Curve c; aluminium

Fig. 6. Angular distribution of backscattered electrons for 30 keV electrons, normal incidence showing evolution with thickness, for aluminium,
Curve a; 1 μm
Curve b; 2 μm
Curve c; 3 μm
Curve d; 5 μm
Curve e; 13 μm

Fig. 7. Angular distributions of backscattered electrons for 30 keV electrons, normal incidence, showing evolution with thickness, for gold,
Curve a; 0.04 μm
Curve b; 0.10 μm
Curve c; 0.16 μm
Curve d; 0.40 μm
Curve e; 0.88 μm

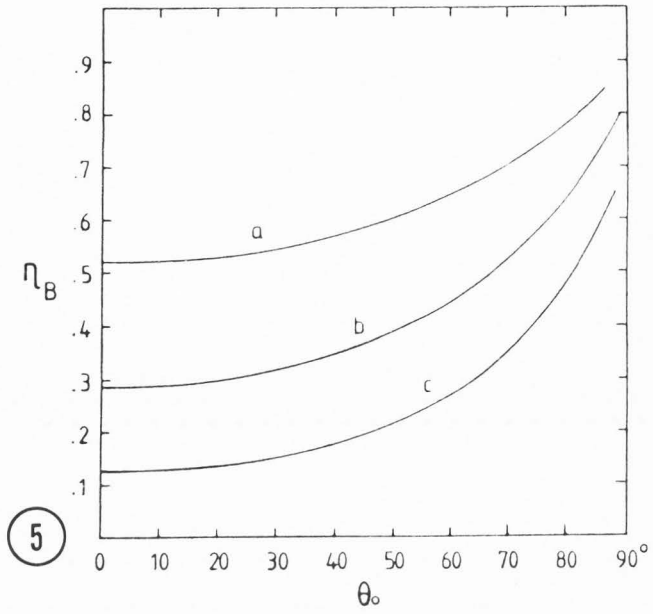

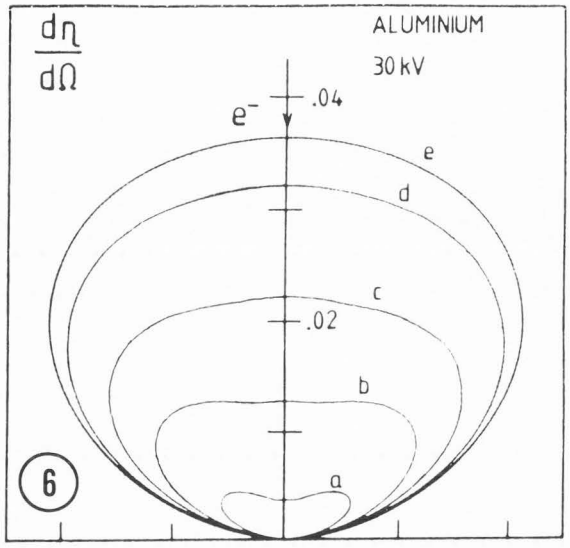

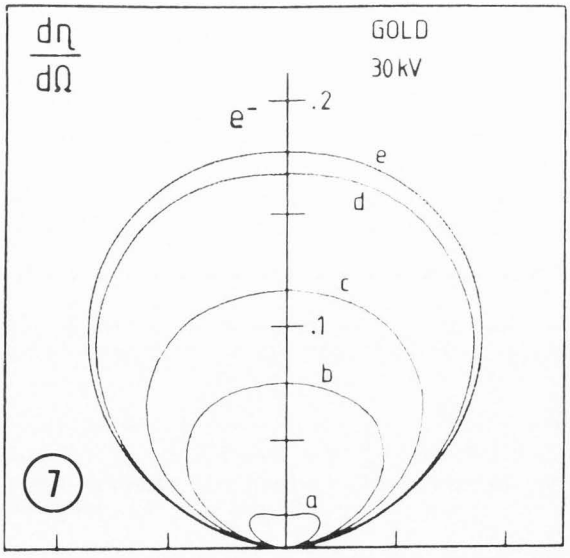

The angular distribution of backscattered electrons $d\eta_B/d\Omega$ was investigated as a function of atomic number Z and target thickness t. Polar plots of angular distributions calculated using the single energy loss approximation are shown in Figures 6, for aluminium and 7, for gold. The calculations were carried out for $E_0 = 30$ keV and $\Theta_0 = 0$. It appears that, for any Z the angular distribution has pronounced lobes for a thickness much less than the electron range, r_B. As the thickness is increased the lobes become less pronounced and the distribution eventually reaches a stationary state characteristic of the bulk for t a little less than 0.5 r_B. For all Z this distribution is approximately cosine being slightly flattened for low Z and slightly elongated for high Z. (Figure 6 curve e and Figure 7 curve e) These dependencies on t and Z can be explained in terms of the average number of elastic scattering events undergone by backscattered electrons (Kanter (1964)). They agree with the experiments of Kanter (1957) except for small t and low Z when Kanter found that the cosine distribution persisted. They are, however, in good agreement with Niedrig's experiments (Niedrig (1978a,b)).

Figure 8 shows polar plots for non-normal incidence calculated using the theory described in Appendix A in which variations with ϕ are included. The elongated lobe in the plane of incidence is as expected and is in agreement with experiments (Seidel (1972)), Reimer et al. (1978)) and Monte-Carlo calculations (Shimizu et al. (1972)).

The more sophisticated theory with more than one energy loss does not make appreciable changes to these results. It is the ratio of inelastic to elastic scattering which mainly determines the features of these distributions.

The transmitted backscattered and absorbed fractions, η_T, η_B and η_A were calculated as functions of target thickness, and the forward and backward travelling fluxes I_F and I_B were calculated as functions of depth z for $t = \infty$ (i.e. bulk target). The calculations were carried out for incident electron energies $E_0 = 10$, 20, 30 and 50 keV for aluminium, copper and gold. The usual scaling with electron range was

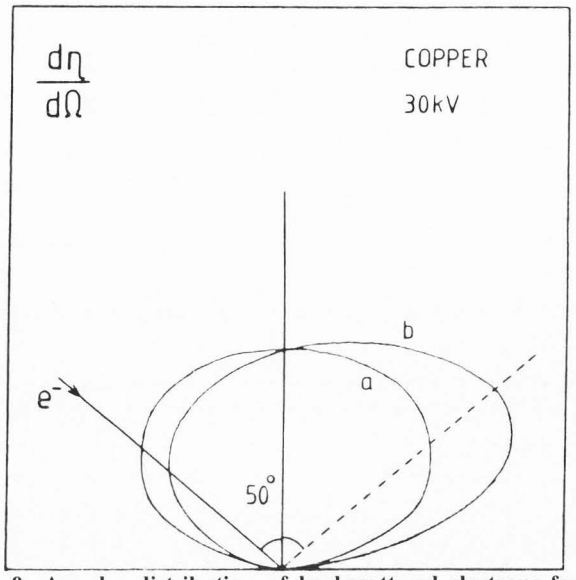

Fig. 8. Angular distribution of backscattered electrons for 30 keV electrons, 50° angle of incidence for copper, Curve a; $\phi = 90°$ Curve b; $\phi = 0°$

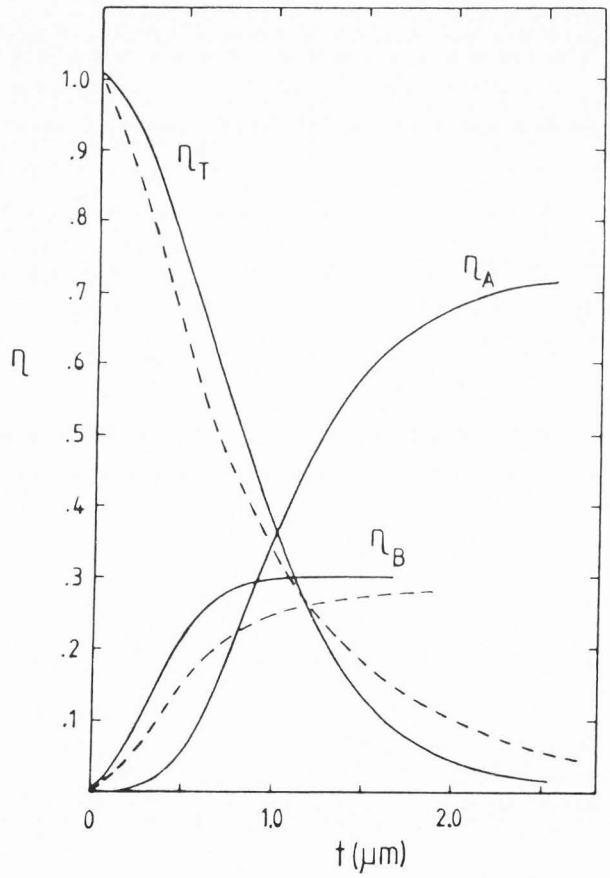

Fig. 9. Transmitted backscattered and absorbed fractions η_T, η_B and η_A versus target thickness t for 30 keV electrons, normal incidence, copper.

found to hold well for each element, particularly for η_T; η_B increasing and η_A decreasing slowly with decreasing incident energy. Figure 9 shows η_T, η_B and η_A for copper, $E_0 = 30$ keV, $\Theta_0 = 0$ calculated using the single loss theory (dashed curves). These curves show the same trends as the experimental ones of Cosslett and Thomas (1965) and Reimer and Drescher (1977). However η_A increases too quickly for small t and η_B too slowly and η_T decreases too slowly for large t. This is to be expected since the rate of absorption in the single loss (N = 1) approximation is too high at high energies characteristic of the distributions at small t and too low for the low energies which are important at large t. This can be corrected by using a larger value of N. The solid curves show the results for N = 10.

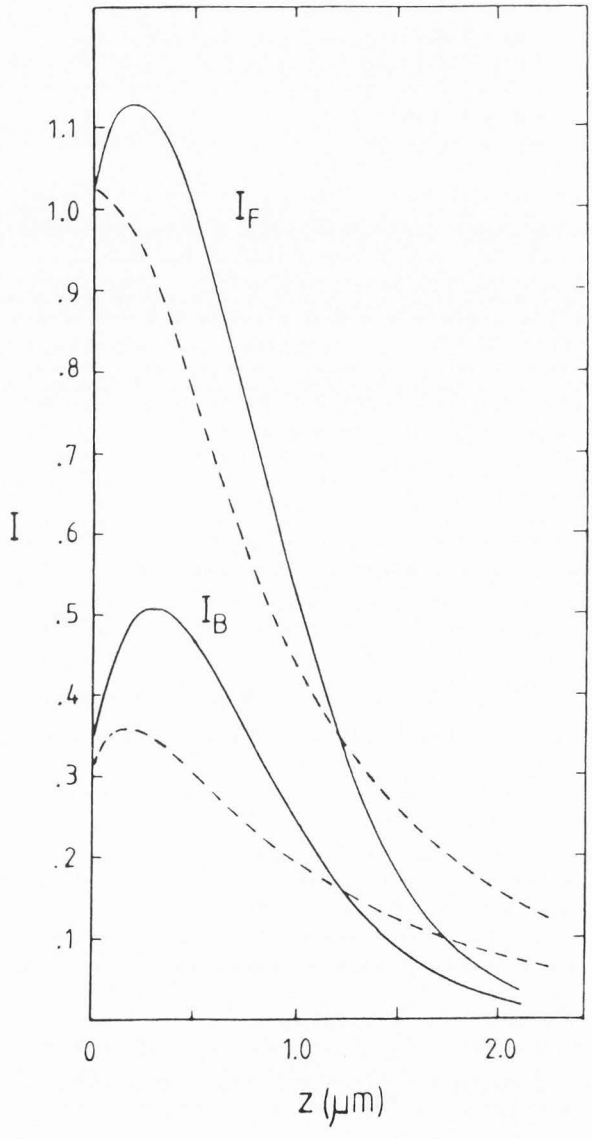

Fig. 10. Forward and backward travelling fluxes I_F and I_B versus depth z in a bulk target of copper ($t = \infty$). Solid curve is for N = 10, dashed curve for N = 1. Incident energy 30 keV.

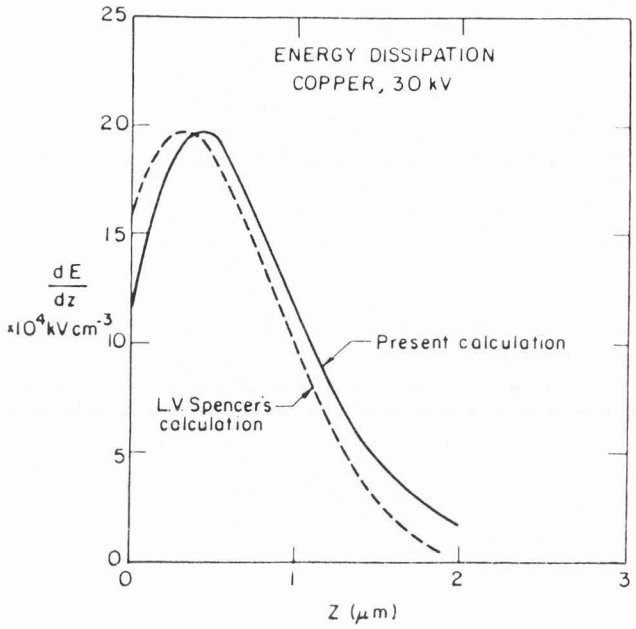

Fig. 11. Energy dissipation dE/dz for 30 keV electrons incident normally on bulk copper.

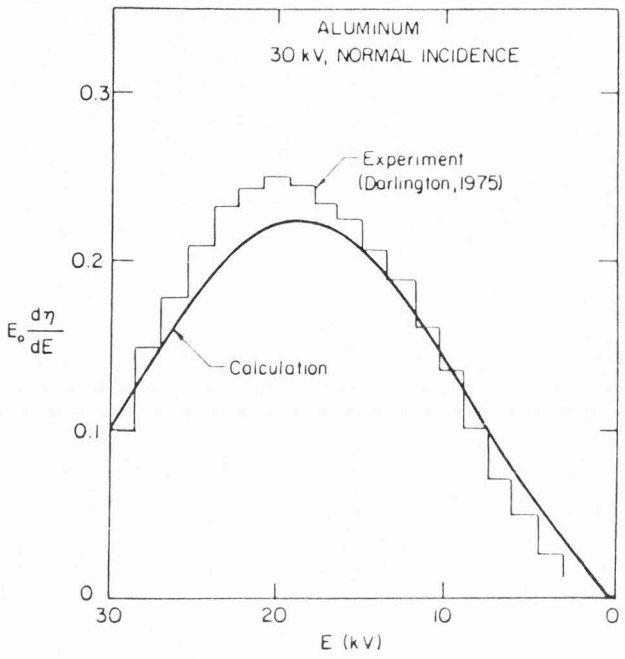

Fig. 12. Energy distribution of backscattered electrons, E_0 30 keV, Θ_0, bulk aluminium.

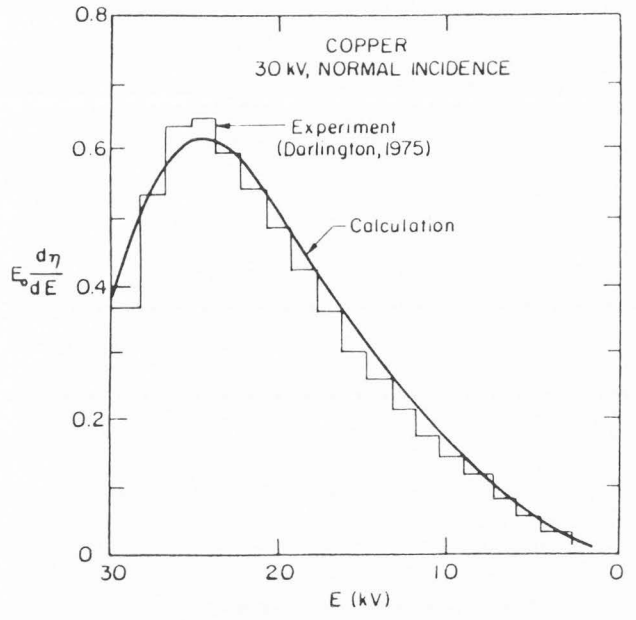

Fig. 13. Electron distribution of backscattered electrons, E_0 = 30 keV, Θ_0 = 0, bulk copper.

Figure 10 shows results for I_F and I_B calculated as functions of z, for t = ∞. These distributions are not directly observable but they are used to calculate other quantities such as X-ray or Auger electron production. The full curves show the results for N = 10 and the dashed curves for N = 1. Both sets of curves were calculated for copper, E_0 = 30 keV, Θ_0 = 0.

The energy dissipated per unit depth dE/dz may be readily calculated from $I_F(z)$ and $I_B(z)$. Figure 11 shows the energy dissipation in copper for 30 keV electrons at normal incidence calculated with 5 energy levels (full curve). It is compared with L.V. Spencer's (1955) calculation of the energy dissipation in an infinite medium for copper at 25 keV, scaled to 30 keV (dashed curve). The discrepancy between the two curves is probably due to the difference in boundary conditions.

The energy distributions of backscattered electrons for aluminium, copper and gold are shown in Figures 12, 13 and 14 and compared with the experimental results of Darlington (1975). The agreement is good. The calculations show a strong dependence on Z. For high Z the distribution has a sharp maximum close to the incident energy E_0. As Z is reduced the maximum becomes much broader and moves to a lower energy. This is a result of the ratio of elastic to inelastic scattering probabilities. For high Z this ratio is relatively large and the probability of electrons being backscattered before losing much energy is high. For low Z this ratio is smaller and electrons are not likely to be backscattered so rapidly. This results in a maximum in the distribution at a lower energy.

This theory can also be used to calculate the production of X-rays. For example the variation of X-ray production with depth is simply

$$\phi(z) = (V1 + V2).\phi.\epsilon\chi\pi - \Lambda z.V2^{-1}.I_{0'} \qquad 42$$

from equations (32). ϕ is the rate at which X-rays are produced per electron normalized to the rate of production in a thin film. A calculation of this function in its usual form $\phi(\varrho z)$ is shown in Figure 15. The agreement with experimental results is good.

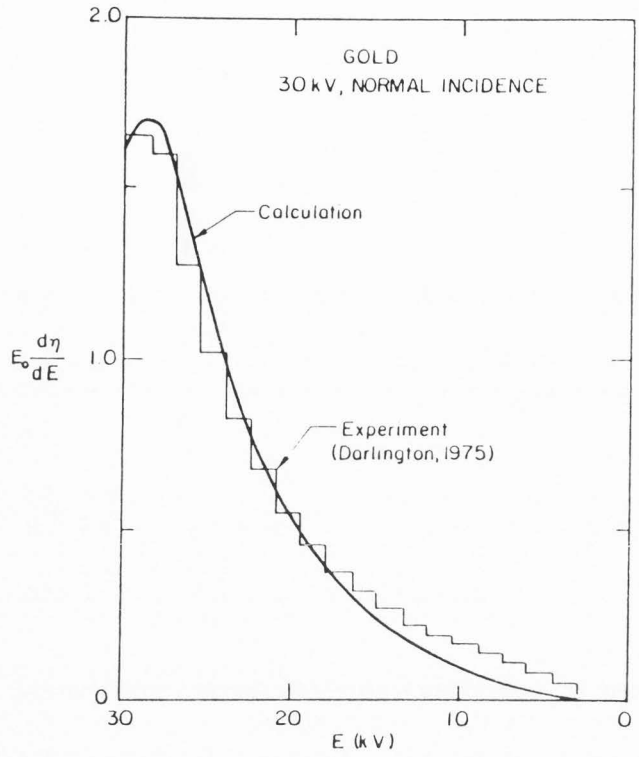

Fig. 14. Electron distribution of backscattered electrons, E_0 = 30 keV, Θ_0, bulk gold.

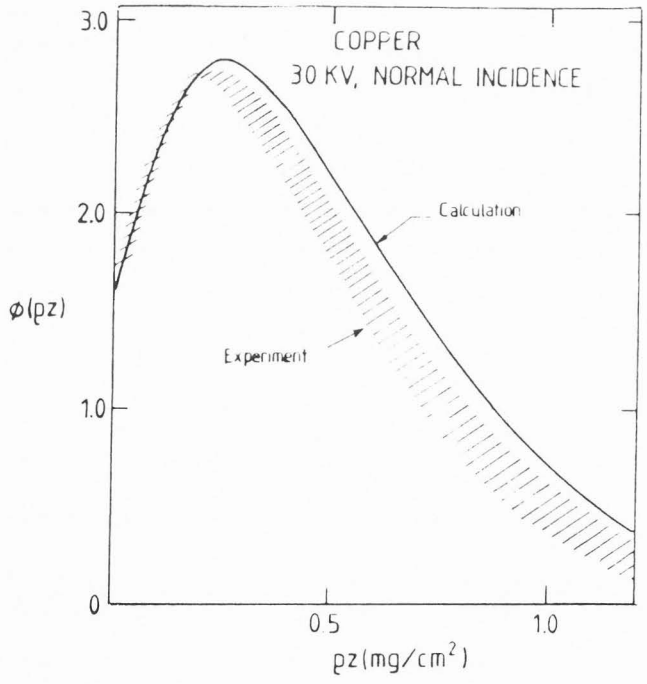

Fig. 15. Depth distribution of Cu Kα X-rays, E_0 = 30 keV, Θ_0 = 0, bulk copper.

However it is usually more convenient to calculate the X-ray yield directly. The total X-ray yield C is obtained by an analytic integration as

$$C = (V1 + V2).\phi.(\Lambda + \mu \sec \Theta_T)^{-1}.V2^{-1}.I_0 \qquad 43$$

where μ is the appropriate X-ray absorption coefficient and Θ_T is the detector take off angle. There is therefore no extra work involved in calculating X-ray yields instead of electron distributions.

Equation (43) has been used as the basis not only for the calculation of X-ray yields but also as a means of determining mass fractions from characteristic X-ray spectra (Fathers and Skarnulis (1980)).

A closely related problem is the calculation of the Auger backscattering factor r which has been discussed in great detail for low incident energies by Shimizu and Ichimura (1981).

By analogy with equation (43), the rate of Auger electron production may be written

$$C = 1 + r \qquad 44$$

where the r accounts for the Auger electrons produced by the backscattered electrons. Then

$$r = \frac{1}{\sec \Theta_0 \, \phi(E_0)} \int \sec \Theta \, \phi(E) \frac{d^2\eta}{d\Theta dE} d\Theta dE \qquad 45$$

(Bishop and Rivière, (1969)).

r has been calculated for a wide range of Auger transitions as a function of incident energy E_0 and incident angle Θ_0. Representative results are shown in Figure 16, for silicon (KLL 1619 eV), copper (LVV 920 eV) and silver (MNN 350 eV).

Detailed understanding of these results is difficult. However, quite crude arguments show that r is approximately $2\eta_B$. $2\eta_B$ for the three examples, at normal incidence is .352, .650 and .824 respectively for a, b and c. In general it seems that r increases slowly with decreasing E_0. The behaviour as a function of Θ_0 is more complex. For low Z r increases with increasing Θ_0, whereas for high Z r decreases with increasing Θ_0. For medium Z ((n)) r shows little variation with Θ_0.

A fuller understanding will require extensive calculations of the distributions of backscattered electrons in energy and angle. This work is in progress in the hope that it will be possible to parameterize these variations of r with E_0, Θ_0 and Z.

CONCLUSIONS

By dividing the transport equation into angle and energy segments, it can be expressed as a set of coupled differential equations which can be solved by the methods outlined above.

The distributions of electrons in energy and angle can be expressed as matrix operators which are analytic functions of depth z and target thickness t. Other quantities of interest such as X-ray or Auger electron production may be similarly calculated.

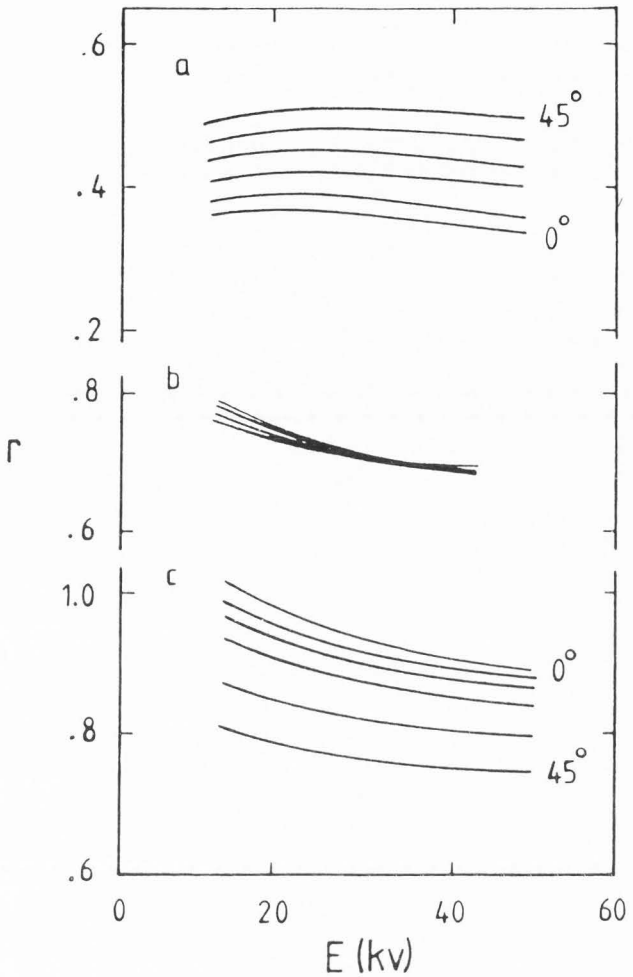

Fig. 16. Auger backscattering factor r versus incident electron energy E for Θ_0 0° → 45°,
Curves a; silicon KLL 1619 eV
Curves b; copper LVV 920 eV
Curves c; silver Mnn 350 eV

A simplified theory with only one energy loss accounts well for the gross variations of backscattering fraction with angle and atomic number. It seems that many of the features of backscattering are related to the ratio of the elastic scattering cross section to the inelastic scattering cross section. This ratio is very nearly proportional to atomic number. Using the simplest version of the theory in which only two directions of scattering are allowed (the forward-backward theory) gives results for η_B as an analytic function z and t. In this case the variation of η_B with atomic number can also be expressed as an analytic expression which has the correct functional form.

The gross features of the energy distributions seem to be described quite well by a relatively simple model in which inelastic scattering can only occur from one energy 'level' to the 'level' immediately below it. The scattering probabilities between levels are determined to preserve the mean rate of energy loss given by the Bethe energy loss law.

Calculations based on the theory are fast and stable and can be carried out without difficulty on a minicomputer. Effects giving rise to small changes in any observable quantity can be calculated accurately using perturbation theory.

ACKNOWLEDGEMENTS

We would both like to thank the Science Research Council, U.K. for financial support during the course of this work.

REFERENCES

Archard GD. (1961). Backscattering of electrons. J. Appl. Phys. **32**, 1505-1509.

Bellman R, Kalaba R and Wing G. (1960). Invariant imbedding and mathematical physics. I. Particle processes. J. Math. Phys. **1**, 280-308.

Bennett AJ and Roth LM. (1972). Effect of primary diffusion on secondary electron emission. Phys. Rev. B **5**, 4309-4324.

Bethe HA, Rose ME and Smith LP. (1938). The multiple scattering of electrons. Proc. Amer. Phil. Soc. **78**, 573-585.

Bishop HE. (1965). A Monte Carlo calculation of the scattering of electrons in copper. Proc. Phys. Soc. **85**, 855-866.

Bishop HE. (1966). Electron scattering and x-ray production. Ph.D. thesis, University of Cambridge, U.K.

Bishop HE and Rivière JC. (1969). Estimates of the efficiencies of production and detection of electron excited Auger emission. J. Appl. Phys. **40**, 1740-1744.

Brown DB and Ogilvie RE. (1966). An electron transport model for the prediction of X-ray production and electron backscattering in electron microanalysis. J. Appl. Phys. **37**, 4429-4433.

Brown DB, Wittry DB and Kyser DF. (1969). Prediction of X-ray production and electron scattering in electron probe analysis using a transport equation. J. Appl. Phys. **40**, 1627-1636.

Case KM and Zweifel LF. (1967). Linear transport theory, published by Addison-Wesley, London, U.K.

Chandrasekhar S. (1950). Radiative transfer, published by Clarendon Press, Oxford, U.K.

Cosslett VE and Thomas RN. (1965). Multiple scattering of 5-30 keV electrons in evaporated metal films. Brit. J. Appl. Phys. **16**, 779-796.

Darlington EH. (1975). Backscattering of 10-100 keV electrons from thick targets. J. Phys. D. **8**, 85-93.

Dashen RF. (1964). Theory of electron backscattering. Phys. Rev. **134**, No. 4a, A1025-A1032.

Everhart TE. (1960). Simple theory concerning reflection of electrons from solids. J. Appl. Phys. **31**, 1483-1490.

Fathers DJ and Rez P. (1979). A transport equation theory of electron backscattering, Scanning Electron Microsc., 1979; I: 55-56.

Fathers DJ and Skarnulis AJ. (1980). The application of standardless X-ray microanalysis to biological material. Proc. Ninth International Conf. on X-ray Optics and Microanalysis, P. Brederoo and V.E. Cosslett (eds.), Seventh

European Congress on Electron Microscopy Foundation, Leiden, 152-153.

Goudsmit S and Saunderson JL. (1940). Multiple scattering of electrons. Phys. Rev. **57**, 24-29.

Jacobs JH. (1973). Multiple electron scattering through a slab. Phys. Rev. A **8**, 226-235.

Jakubovics JP and Fathers DJ. (1978). Image profiles and resolution of magnetic domains in the scanning electron microscope. Phys. Stat. Sol. **46a**, 291-303.

Kanaya K and Ono S. (1978). The energy dependence of a diffusion model for an electron probe into solid targets. J. Phys. D. **11**, 1495-1508.

Kanter H. (1957). The backscattering of electrons in the energy range 10 keV to 20 keV. Ann. Phys. (Leipzig) **20**, 144-146.

Kanter H. (1964). Backscattering of kilovolt electrons from thin films. Brit. J. Appl. Phys. **15**, 555-559.

Lewis HW. (1950). Multiple scattering in an infinite medium. Phys. Rev. **78**, 526-529.

Liljequist D. (1977). A simple analysis of the transmission and backscattering of 10-30 keV electrons in solid layers. J. Phys. D.**10**, 1363-1377.

Niedrig H. (1978a). Physical background of electron backscattering. Scanning **1**, 17-34.

Niedrig H. (1978b). Backscattered electrons as a tool for film thickness determination, Scanning Electron Microsc., 1978; I: 841-858.

Reimer L and Drescher H. (1971). Secondary electron emission of 10-100 keV electrons from transparent films of aluminium and gold. J. Phys. D. **10**, 805-815.

Reimer L, Popper W and Bracker W. (1978). Experiments with a small angle detector for backscattered electrons, Scanning Electron Microsc., 1978; I: 705-710.

Reimer L and Krefting ER. (1975). The effect of scattering models on the results of Monte Carlo calculations, in: Use of Monte Carlo Calculations in Electron Probe Microanalysis, K. Heinrich, H. Yakowitz, D.E. Newbury (eds.), NBS Special Publication 460, Washington, DC, 45-60.

Seidel H. (1972). Messungen zum Rückstreu- und Transmissionskoeffizienten an polykristallinem Material und zur Orientierungsanisotropie des Rückstreukoeffizienten und der Sekundärelektronenausbeute für 9 bis 100 keV-Elektronen. Doctoral Thesis, Universitat Münster (quoted by Niedrig (1978)).

Shimizu R, Ikuta T and Murata K. (1972). The Monte Carlo technique as applied to the fundamentals of EPMA and SEM. J. Appl. Phys. **43**, 4233-4249.

Shimizu R and Ichimura S. (1981). Quantitative analysis by Auger electron spectroscopy – Monte Carlo calculations of electron backscattering effects. Toyota Foundation Research Report No. I-006 76-0175. (Available from Prof. R. Shimizu, Dept. Appl. Phys., Osaka Univ., Osaka 565, Japan).

Spencer JP, Humphreys CJ and Hirsch PB. (1972). A dynamic theory for the contrast of perfect and imperfect crystals in the scanning electron microscope using backscattered electrons. Phil. Mag. **26**, 193-213.

Spencer JP. (1974). Diffraction contrast in the scanning electron microscope. D. Phil. Thesis, University of Oxford.

Spencer JP and Humphreys CJ. (1980). A multiple scattering transport theory for electron channelling patterns. Phil. Mag. A **42**, 433-451.

Spencer LV. (1955). Theory of electron penetration. Phys. Rev. **98**, 1597-1615.

Strickland DJ and Bernstein IB. (1976). Angular properties of particle fluxes for strongly forward peaked scattering. J. Appl. Phys. **47**, 2184-2190.

Wang MC and Guth E. (1951). On the theory of multiple scattering, particularly of charged particles. Phys. Rev. **84**, 1092-1111.

APPENDIX A

The differential scattering cross section σ and the electron flux I are expanded into Fourier series:

$$I(z,\Theta,\phi,E) = \Sigma_{-\infty}^{\infty} B_m(z,\Theta,E)\exp im\phi \qquad (A1)$$

and $$\sigma(\phi,\Theta,E;\phi',\Theta',E') = \Sigma_{-\infty}^{\infty} D_p(\Theta,E\Theta',E') \exp ip(\phi - \phi') \qquad (A2)$$

where $$D_p = \frac{1}{2\pi} \int_{-\pi}^{\pi} \sigma(\phi,\Theta,E;\phi',\Theta',E') \exp ip(\phi - \phi')\, d(\phi - \phi') \qquad (A3)$$

Then equation (2) can be written

$$\cos\Theta = \frac{d}{dz} \Sigma B_m \exp im\phi$$
$$= \int [\Sigma D_p' \exp ip(\phi - \phi') \Sigma B_m' \exp im\phi - \Sigma D_p \exp ip(\phi - \phi) \Sigma B_m \exp im\phi] \sin\Theta'\, d\phi'\, d\Theta'\, dE' \qquad (A4)$$

where

$$B_m = B_m(z,\Theta,E)$$
$$B_m' = B_m(z,\Theta',E')$$
$$D_p' = D_p(\Theta,E;\Theta',E')$$
$$D_p' = D_p(\Theta',E';\Theta,E) \qquad (A5)$$

Carrying out the integration over ϕ' and equating coefficients of the exp $im\phi$ gives

$$\cos\Theta \frac{dB_m}{dz} = \int (D_m B_m - D_0' B_m') \sin\Theta' \, d\Theta' \, dE' \quad (A6)$$

This equation is solved for any m in the same way as the equation for B_0. This solution is derived in the text.

APPENDIX B

The present solution for backscattered electron flux for a semi-infinite target is, from equation (32),

$$I_B(0) = V1 . V2^{-1} . I_0 \quad (B1)$$

Therefore the reflection operator R can be written

$$R = V1 . V2^{-1} \quad (B2)$$

In this appendix it is shown that this is also a solution of Dashen's non linear matrix equation (23). Substituting in (23) gives

$$A_B + A_F V1 . V2^{-1} A_F + V1 . V2^{-1} . A_B V1 . V2^{-1} \quad (B3)$$

From the definition of V1, V2 we have

$$\begin{pmatrix} A_F & A_B \\ -A_B & -A_F \end{pmatrix} \begin{pmatrix} V1 & V2 \\ V2 & V1 \end{pmatrix} =$$

$$\begin{pmatrix} V1 & V2 \\ V2 & V1 \end{pmatrix} \begin{pmatrix} \lambda & 0 \\ 0 & -\lambda \end{pmatrix}$$

Thus

$$A_F V1 + A_B V2 = V1\lambda$$

$$A_F V2 + A_B V1 = -V2\lambda \quad (B4)$$

and

$$A_F V1 = V1\lambda - A_B V2$$

$$A_B V1 = 1V2\lambda - A_F V2$$

Substituting for these quantities in B3 gives

$$A_B + V1\, V2^{-1} - A_B + V1V2^{-1}A_F$$

$$- V1\, V2^{-1} - V1V2^{-1} A_F$$

which is identically zero as required.

APPENDIX C

Simple Forward Backward Theory

In this case the scattering matrix is 2 × 2,

$$A = \begin{pmatrix} -\mu & r \\ -r & \mu \end{pmatrix} \quad (C1)$$

where r is the reflection coefficient, a is the absorption coefficient and $\mu = r + a$. The transport equation may be written

$$\frac{dI_F}{dz} = -\mu I_F + r I_B$$

$$\frac{dI_B}{dz} = -r I_F + \mu I_B \quad (C2)$$

where I_F and I_B are the forward and backward travelling currents respectively.

From (C2) by differentiating we obtain

$$\frac{d^2 I_F}{dz} = (\mu^2 - r^2) I_F$$

and

$$\frac{d^2 I_B}{dz} = (\mu^2 - r^2) I_B \quad (C3)$$

with solutions,

$$I_F = A \exp \lambda z + B \exp(-\lambda z)$$

$$I_B = C \exp \lambda z + D \exp(-\lambda z) \quad (C4)$$

and where $\lambda^2 = \mu^2 - r^2$.

The boundary conditions are

$$I_F(0) = I_0$$

$$I_B(t) = 0 \quad (C5)$$

and from equations (C2), (C5) we determine A,B,C and D.

The results are:

$$(C - D) = \frac{r . I_0}{\lambda + \mu \tanh \lambda t}$$

$$(C + D) = \frac{r \tanh \lambda t . I_0}{\lambda + \mu \tanh \lambda t}$$

$$(A + B) = I_0$$

$$(A - B) = -\frac{(\lambda \tanh \lambda t - \mu) . I_0}{\lambda + \mu \tanh \lambda t} \quad (C6)$$

and for the electron currents, from C4

$$I_F(z,t) = \frac{\lambda \cosh \lambda(t - z) + \mu \sinh \lambda(t - z)}{\lambda \cosh \lambda t - \mu \sinh \lambda t} . I_0$$

$$I_B(z,t) = \frac{r \sinh \lambda(t - z)}{\lambda \cosh \lambda t + \mu \sinh \lambda t} \quad \text{(C7)}$$

Similar methods may be used for the case with several angular segments, however the matrix algebra is complex and will not be given here. The general method is outlined in the text. The importance of these results is in the way they illustrate certain trends in terms of analytic expressions.

Consider the variation of backscattered electron current with $\Sigma = {}^{a}/_{r}$. First of all, from (C7), with some manipulations, we obtain

$$I_B(0,\infty) = 1 + \Sigma - \sqrt{(1 + \Sigma)^2 - 1} \quad \text{(C8)}$$

The values of r and a may be estimated as follows. The reflection coefficient is obtained by integrating the Rutherford differential scattering cross section over the backward hemisphere,

$$r = \frac{\pi Z^2 e^4}{4E_0^2} \quad \text{(C9)}$$

and evaluating the absorption coefficient a so that the mean rate of energy loss is that given by the Bethe law, gives,

$$a = \frac{2\pi Z e^4}{E_0^2} \log\left(\frac{1.166\, E_0}{J}\right) \quad \text{(C10)}$$

From C9 and C10,

$$\Sigma = \frac{8C}{Z}, \text{ where } C = \log\left(\frac{1.166\, E_0}{J}\right)$$

where Z is atomic number, E_0 is the incident electron energy and J is the mean ionization potential. Equation C8 therefore gives an expression for the variation of backscattering with atomic number in a closed analytic form, which may be compared with the more sophisticated calculation in the text.

APPENDIX D

The solution of the many energy level (or multi group) supermatrix differential equation proceeds in a similar way to the one level problem. The diagonalization of the supermatrix is achieved in stages. First the supermatrix may be put into block diagonal form by determining the matrices T which satisfy the equation,

$$\begin{pmatrix} A^{00} & 0 & 0 \\ A^{10} & A^{11} & 0 \\ 0 & A^{21} & A^{22} \end{pmatrix} \begin{pmatrix} T_{11} & 0 & 0 \\ T_{21} & T_{22} & 0 \\ T_{31} & T_{32} & T_{38} \end{pmatrix} = \begin{pmatrix} T_{11} & 0 & 0 \\ T_{21} & T_{22} & 0 \\ T_{31} & T_{32} & T_{33} \end{pmatrix} \begin{pmatrix} A^{00} & 0 & 0 \\ 0 & A^{11} & 0 \\ 0 & 0 & A^{22} \end{pmatrix} \quad \text{(D1)}$$

which is similar to a conventional eigenvalue equation except that the elements are themselves matrices. The matrices T are found by solving equations of the following form, column by column

$$A^{00} T_{11} = T_{11} A^{00}$$

$$A^{10} T_{11} + A^{11} T_{21} = T_{21} A^{00} \quad \text{(D2)}$$

The diagonal terms may be taken as the unit matrix E without any loss of generality. The eigenvalues of the supermatrix are the eigenvalues of the diagonal matrices A^{mm} and the eigenvector supermatrix V is the product of the lower triangular T supermatrix and the eigenvectors X of the A^{mm}, i.e.

$$\begin{pmatrix} V_{11} & 0 & 0 \\ V_{21} & V_{22} & 0 \\ V_{31} & V_{32} & 0 \end{pmatrix} = \begin{pmatrix} E & 0 & 0 \\ T_{21} & E & 0 \\ T_{31} & T_{32} & E \end{pmatrix} \begin{pmatrix} X_0 & 0 & 0 \\ 0 & X_1 & 0 \\ 0 & 0 & X_2 \end{pmatrix}$$

where $A^{mm}X_m = X_m \Lambda_m$ (D4)

A recurrence scheme is used to calculate all the component matrices which minimizes computer time and storage.

Partitioning into forward and backward scattering is carried out in an analogous way to the single level theory and solutions formally identical to equations (31) and (32) are obtained except that the matrices have the lower triangular structure of the eigenvector matrix derived above. This structure is a consequence of the fact that electrons can only lose energy through inelastic scattering. It considerably simplifies the solution.